Temperature- and field-induced structural transitions in magnetic colloidal clusters

J. Hernández-Rojas

Departamento de Física and IUdEA, Universidad de La Laguna, 38205, La Laguna, Tenerife, Spain

F. Calvo

Laboratoire Interdisciplinaire de Physique, Université Grenoble Alpes and CNRS, 140 Av. de la physique, 38402 St Martin d'Hères, France

Magnetic colloidal clusters can form chain, ring, and more compact structures depending on their size. In the present investigation we examine the combined effects of temperature and external magnetic field on these configurations by means of extensive Monte Carlo simulations and a dedicated analysis based on inherent structures. Various thermodynamical, geometric, and magnetic properties are calculated and altogether provide evidence for possibly multiple structural transitions at low external magnetic field. Temperature effects are found to overcome the ordering effect of the external field, the melted stated being associated with low magnetization and a greater compactness. Tentative phase diagrams are proposed for selected sizes.

I. INTRODUCTION

Assemblies of finite dipolar particles ranging from nano- to meso- and even macroscopic scales exhibit collective properties and a propensity for self-assembly that has motivated an increasing number of investigations in recent years [1–29].

On the experimental side, Zerrouki and coworkers designed magnetic colloids that self-assemble with a well-defined helicity [30], a feature also reported for magnetite nanocubes [23]. The structure and dynamics of self-assembled colloidal clusters have been observed by isolating the particles in microwells with the purpose of obtaining ensemble-averaged probabilities of cluster structures as a function of the number of colloidal particles [31]. Macroscopic mechanical properties of self-assembled ferromagnetic spheres have been studied by Vella and coworkers [32], who obtained chains, rings, and cylinders as the main structural motifs. Branched structures have also been observed [2]. Other experimental investigations on the structure, thermodynamics and kinetics of colloidal magnetic clusters have been carried over the past few years [33–36], revealing nontrivial shapes and collective phenomena engineered by specific design protocols of the particles themselves and by appropriate tuning of the external experimental conditions.

From the theoretical point of view, Vandewalle and Dorbolo [37] obtained from numerical simulations mechanically stable defects that appeared to behave as macroscopic magnetic monopoles. In a recent work, Messina and coworkers [22,24,28] located low-energy structures for finite sets of spherical magnetic particles in two and three dimensions. These structures were experimentally reproduced with millimeter-scale magnets. A popular theoretical framework for magnetic nanoparticles is the dipolar hard sphere (DHS) model in which the permanent dipole moment is fixed at the center of a hard sphere. The DHS model has been extensively employed due to its simplicity by various groups [38,39]. It notably

supports ring and chain structures, as observed experimentally for spherical magnetic particles [1,6,7,9]. Alternative continuous models involving a soft repulsive core that is more appropriate for dynamical studies have also been considered recently by Novak and coworkers [29], who specifically investigated the effects of magnetic dipole strength on the preferential formation of chains or ring structures.

An external magnetic field can strongly alter the shape of magnetic colloidal clusters, as demonstrated experimentally under a variety of conditions [2,11,18,23]. In particular, Kun and coworkers [2] have investigated for clusters of 10–20 colloidal particles the breakup of ring structures into chains as the external field is increased above about 50 Gauss. Similar studies by Morimoto and coworkers have focused on two-dimensional assemblies [8,15] for particles with centered dipoles. In contrast, when the dipole moments are off-centered, a recent investigation has revealed hierarchical self-assembly into reconfigurable shells [25]. Nontrivial structures have also been predicted to occur in the presence of a time-dependent external field [12,16,21]. Static external fields were found to alter the energy landscapes and entire rearrangement pathways for a simple model of colloidal magnetic particles that includes a short-ranged depletion interaction [40].

Besides the model details, the preferred structures of magnetic colloidal clusters appear to depend on temperature, external field, and size itself. In the present contribution, we attempt to rationalize this complex dependence by carrying out extensive exchange Monte Carlo simulations. In addition to generic indicators related to the thermodynamical or structural state of the clusters, we have also considered transitions affecting fluxionality in the energy landscapes and based on inherent structures. Combining these indicators, phase diagrams are proposed for various cluster sizes, often revealing multiple structural transitions that could be exploited to design desired shapes by tuning temperature or field strength.

This paper is organized as follows. The basic methods, including the model details and the computational protocol, are described in Sec. II. The results are presented and discussed in Sec. III, before some concluding remarks are finally given in Sec. IV.

II. METHODS

A. Magnetic colloidal clusters

We consider a set of N identical colloidal magnetic particles interacting with each other and with a possible external magnetic field $\vec{B}$ at prescribed temperature T. The potential energy of this system reads [40]

$$V(\mathbf{R}) = V_0(\mathbf{R}) - \vec{\mu}(\mathbf{R}) \cdot \vec{B}, \qquad (1)$$

where $V_0(\mathbf{R})$ is the binding energy and $\vec{\mu}(\mathbf{R})$ the total magnetic dipole moment,

$$\vec{\mu}(\mathbf{R}) = m \sum_i \hat{\boldsymbol{u}}_i, \qquad (2)$$

m being the strength of the magnetic dipole moment carried by each particle and $\hat{\boldsymbol{u}}_i$ the unit vector carrying this dipole moment for particle i.

In Eq. (1), V_0 comprises two terms, namely a dipole-dipole interaction contribution and a (mostly repulsive) Morse pairwise potential preventing the collapse at short distances, given by

$$V_0(\mathbf{R}) = \sum_{i<j}^N V_0(r_{ij}) = \sum_{i<j}^N [V_M(r_{ij}) + V_{\text{dip}}(r_{ij})], \qquad (3)$$

where the Morse pair potential V_M is expressed as

$$V_M(r_{ij}) = \varepsilon e^{\rho(1-r_{ij}/\sigma)}[e^{\rho(1-r_{ij}/\sigma)} - 2], \qquad (4)$$

and the dipole-dipole interaction can be written as

$$V_{\text{dip}}(r_{ij}) = \frac{\mu_0}{4\pi} \frac{m^2}{r_{ij}^3}[(\hat{\boldsymbol{u}}_i \cdot \hat{\boldsymbol{u}}_j) - 3(\hat{\boldsymbol{u}}_i \cdot \hat{\mathbf{r}}_{ij})(\hat{\boldsymbol{u}}_j \cdot \hat{\mathbf{r}}_{ij})], \qquad (5)$$

$r_{ij} \equiv |\mathbf{r}_{ij}| = |\mathbf{r}_i - \mathbf{r}_j|$ being the distance between particles i and j, ε the well depth, r_e the equilibrium distance for the pure Morse contribution, and μ_0 the permeability of vacuum. ε and σ are the units of energy and distance, respectively, and $\hat{\boldsymbol{r}}_{ij} = \mathbf{r}_{ij}/r_{ij}$.

The Morse contribution contains one adjustable parameter, ρ, which determines the range of the potential. Following our recent study [40] we used $\rho = 30$ and $m = 4.4$, in reduced units. For possible experimental comparison, it is important to convert such abstract units into physically meaningful quantities. We can safely assume colloidal particles to have a typical radius of $r_0 \sim 1~\mu$m. We then distinguish two situations, in which the magnetic energy for two particles in contact is either of the order of thermal energy at room temperature ($k_B T \sim 4 \times 10^{-21}$ J) or, as in the experimental setup of Wen et al. [1], much larger ($K_{dd} \times k_B T$ with $K_{dd} = 1.7 \times 10^6$ yields an energy of 7×10^{-15} J). In our model, the energy scale at the minimum is about -40ε, which gives values of ε of the order of 10^{-22} J or 2×10^{-16} J, respectively or, in temperature scales, 10 K or 2×10^7 K.

The magnetic dipole moment corresponding to such particles and the associated energy scales is then evaluated

as 2×10^{-16} Am^2 and 3×10^{-13} Am^2, respectively, which yields the scales of magnetic fields to be of the order of 0.2 and 230 Gauss, respectively, both within the experimental reach [2,11,18,23].

Cluster sizes of 8, 14, 21, and 27 particles were chosen as representative samples covering different situations in which the most stable structures evolve from circular rings to linear chains or stacked rings [10,19,40]. In particular, the sizes of 14 and 27 are the lowest at which double and triple ring structures become more stable, respectively, the other two sizes being representative of more generic systems.

B. Finite-temperature sampling under external field

The structural, thermodynamical, and magnetic properties of colloidal clusters were computationally investigated using the exchange (or parallel tempering) Monte Carlo method [41], in which several canonical trajectories are run in parallel and two configurations from adjacent trajectories occasionally swapped with each other. Random moves thus include normal perturbations in the coordinates of a random particle (both in translation and orientation of the dipole moment vector), as well as exchanges between two such configurations. This parallel tempering strategy is mainly employed to reduce broken ergodicity in the simulation and probe possible structural transitions that would hardly be accessible in conventional molecular dynamics or Monte Carlo simulations. For these simulations, the orientational degrees of freedom were treated using simple unit vectors $\hat{\boldsymbol{u}}_i$.

Because the potential is very short ranged (high value of ρ), particles might easily dissociate from the cluster at high or even moderate temperatures, and to keep the clusters connected we have used a simple distance criterion, rejecting Monte Carlo moves in which a particle could become distant from the remaining particles by a unit distance of more than 1.6.

In the presence of an external field, the system loses rotational invariance and it would be possible to introduce global rotational moves in the set of Monte Carlo trial moves or, equivalently, to treat the field orientation as an additional variable. Alternatively, we can integrate what would be the energy at temperature T if an infinite number of such moves were attempted, and the result is a temperature-dependent effective potential in which the magnetic contribution is canonically averaged over all field directions [42]:

$$V_{\text{eff}}(\mathbf{R}; T) = V_0(\mathbf{R}) - \mu(\mathbf{R})B\mathcal{L}[\mu(\mathbf{R})B/k_B T], \qquad (6)$$

where $\mu(\mathbf{R})$ denotes the magnitude of the magnetic dipole vector $\vec{\mu}$, and $\mathcal{L}(x)$ is the Langevin function,

$$\mathcal{L}(x) = \frac{\exp(x) + \exp(-x)}{\exp(x) - \exp(-x)} - \frac{1}{x}. \qquad (7)$$

Under a temperature-dependent potential $V(T)$, the thermodynamical properties such as the internal energy $U(T)$ and heat capacity $C_v(T)$ must explicitly include additional corrections, and we provide below the general expressions for arbitrary V,

$$U(T) = \left\langle V + \beta \frac{\partial V}{\partial \beta} \right\rangle, \qquad (8)$$

and

$$C_v(T) = \frac{1}{k_B T}\left[\langle V^2\rangle - \langle V\rangle^2 + 2\beta\left\langle V\frac{\partial V}{\partial\beta}\right\rangle\right.$$

$$+ \beta^2\left\langle\left(\frac{\partial V}{\partial\beta}\right)^2\right\rangle - \beta^2\left\langle\frac{\partial V}{\partial\beta}\right\rangle^2$$

$$\left. - 2\beta\langle V\rangle\left\langle\frac{\partial V}{\partial\beta}\right\rangle - 2\left\langle\frac{\partial V}{\partial\beta}\right\rangle - \beta\left\langle\frac{\partial^2 V}{\partial\beta^2}\right\rangle\right], \quad (9)$$

where $\beta = 1/k_B T$, k_B being the Boltzmann constant. For the present potential, the derivatives $\partial V/\partial\beta$ and $\partial^2 V/\partial^2\beta$ can be straightforwardly obtained from the explicit form of the Langevin function.

C. Inherent structures analysis

The exchange Monte Carlo simulations provide equilibrated samples from which structural and thermodynamical but also magnetic properties can be determined. We have further supported these analyses by considering the inherent structures (IS's) obtained by locally minimizing the configurations visited by the various trajectories. Doing so periodically provides a way of removing the thermal noise and achieving a closer connection between properties and the underlying structures in the energy landscape [43].

At each temperature, instantaneous configurations are locally optimized using the limited-memory Broyden-Fletcher-Goldfarb-Shanno method [44,45] and treating now the orientational degrees of freedom using an angle-axis coordinate system [46]. Since the Monte Carlo simulations described in the previous section ignore the direction of the finite external field, it was assumed during each minimization that the magnetization vector μ was aligned with the field $\vec{B}$, hence facilitating local optimization in particular toward global rotational degrees of freedom. The set of inherent structures with energies $\{E_\alpha\}$ were recorded and counted, each inherent structure α being found with probability p_α. The amount of fluxionality in the energy landscape can be measured from these statistics, and in the present work we have used the inherent structure entropy S_{IS}, which is just the information entropy associated with the probabilities $\{p_\alpha\}$ as

$$S_{\mathrm{IS}}(T) = -k_B \sum_\alpha p_\alpha \ln p_\alpha. \quad (10)$$

With this definition, a system completely localized into a single structure has a zero entropy, whereas highly fluxional states visiting many inherent structures would have a high value of S_{IS}. The inherent structure entropy is thus likely to be very sensitive to the presence of structural transitions where a limited number of conformers compete with each other.

III. RESULTS AND DISCUSSION

To characterize the equilibrium properties of magnetic colloidal clusters, three main quantities were determined from our exchange Monte Carlo simulations. The canonical heat capacity provides the most fundamental thermodynamical observable that is expected to carry signatures of phase changes rounded by finite-size effects. Structural and magnetic properties more closely connected to the underlying geometric arrangement of the cluster and the collective orientation of the
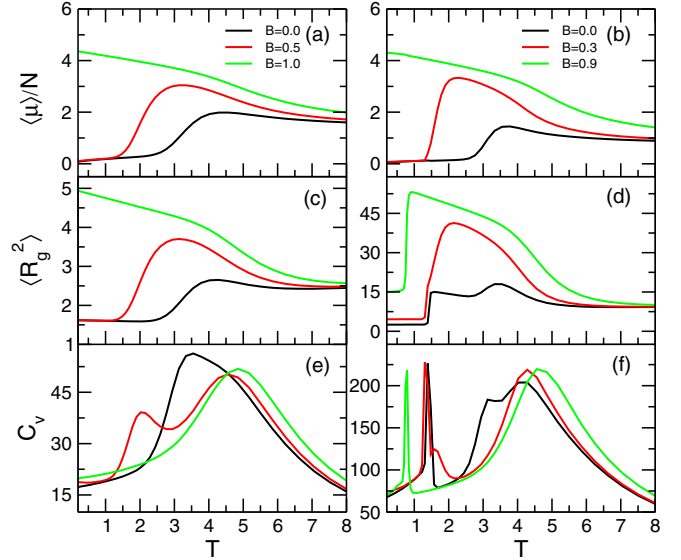
FIG. 1. Equilibrium properties of the M_8 (left panels) and M_{27} (right panels) colloidal clusters as a function of canonical temperature for three values of the external magnetic field B. [(a) and (b)] Average magnetization per particle; [(c) and (d)] average square gyration radius; [(e) and (f)] heat capacity.

dipole moments were also considered, with the square gyration radius R_g^2 and the total magnetization per particle, respectively.

These properties are represented in Fig. 1 for the 8- and 27-particle colloidal clusters, as a function of temperature in the range $T < 8$ reduced units where structural transitions take place. For each system, the results are shown without any external field and for two finite values of the field strength. Besides some size-specific features, several generic remarks can be made. At low temperature and low field the two clusters form one (M_8) or three stacked rings (M_{27}) with zero net dipole and are rather compact. All three indicators considered in Fig. 1 display low values under such conditions. At high field, the clusters preferentially adopt chain conformations in order to maximize their interaction with the field at the expense of intracluster binding, with both gyration radius and magnetization showing now high values at low temperature.

At very high temperatures, the disordering effect of entropy prevails over the ordering role of the external field, and both the magnetization and gyration radius converge to a common value independent of the field, the heat capacity decreasing smoothly back to values comparable to the number of degrees of freedom. This notably indicates that the variety of conformations at very high temperatures encompass chains, rings, and many intermediate structures but no major role played by the lowest-energy conformer.

As temperature increases at low field, the clusters exhibit a single broad melting peak (M_8) or multiple features (M_{27}) in the heat capacity, with possibly sharp additional peaks or low-temperature shoulders. For both systems the average magnetization is only sensitive to the main peak, which is located near the reduced temperature of 3.5–4 reduced units, thus indicating that features below this melting range involve compact structures with low net dipole. For M_{27}, the gyration radius exhibits a correspondingly sharp increase at
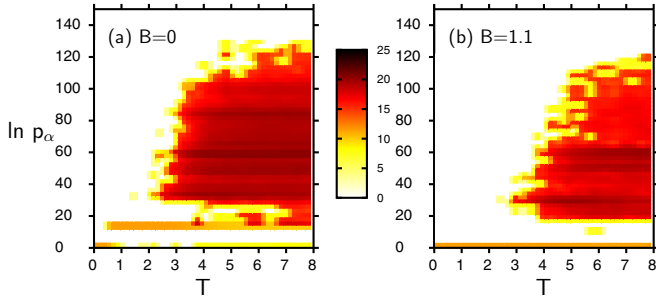
FIG. 2. Probability of visiting inherent structures as a function of their energy and temperature, as explored during the exchange Monte Carlo trajectories for the M_{14} colloidal cluster at two values of the external field. (a) $B = 0$; (b) $B = 1.1$. A logarithmic scale is used for the probability, and all energies are reported relative to the corresponding global minimum energy at each value of the field.

the same temperature as the heat capacity peak near $T = 1.5$ reduced units, showing that this transition is associated with stabilization of more extended but still ringlike conformers.

Under high external fields, the low temperature conformers have all individual dipoles aligned with the field and a net magnetization equal to $m = 4.4$ units. However, structural transitions still occur involving the nonmagnetic degrees of freedom, and the melting transition is preserved, its location not depending significantly on the field magnitude. Even at high fields, premelting transitions occur and can be quite sharp, as in the case of M_{27} near $T = 1$ reduced units and $B = 0.9$. Under such conditions the cluster undergoes a transition to a much less compact state but again without any marked signature on the magnetization. At moderate fields, variations in the relative stability of various conformers affect the caloric curve and the statistical properties, possibly producing additional features that are absent both at low and high fields. For instance, the M_8 cluster at $B = 0.5$ distinctly shows a premelting feature near $T = 2$ reduced units associated with an occasional opening of the ring that is conveyed by the dual increase in the gyration radius and magnetization.

In order to shed more light onto the conformers associated with the various phases, and to characterize the structural transitions and the melted state in greater detail, the inherent structures were determined from instantanous configurations sampled by the exchange Monte Carlo simulations, and their probability $p(E_{IS})$ was accumulated and binned as a function of energy relative to the global minimum. As an example, we show in Fig. 2 the variations of this quantity, in logarithmic scale, as obtained for the M_{14} colloidal clusters at zero and high ($B = 1.1$) field and as a function of temperature. At zero field, this cluster is most stable as a stacked double ring, but undergoes a structural transition toward a single 14-particle ring at low temperature $T \simeq 0.6$. This entropy-driven transition is manifested on the IS spectrum as a conformer lying about 15 energy units above the global minimum. Between this temperature and $T \simeq 3$ units, these two conformers constitute the entire population of minima that are visited in the energy landscape. Above $T = 3$, large bunches of isomers become accessible, and the majority of IS that reach about 110 energy units are visited once temperature approaches $T = 4$ reduced units.
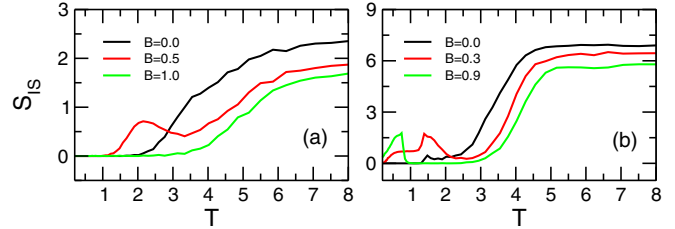
FIG. 3. Information entropy (in units of k_B) inferred from the populations of inherent structures visited in the exchange Monte Carlo simulations, as a function of temperature and for three values of the external magnetic field. (a) M_8; (b) M_{27}.

In contrast, the same system under high external field displays fewer minima with a single, well-defined structure (the linear chain global minimum) until the temperature reaches $T = 3$ units. The remaining excited minima are still numerous but appear at slightly higher temperature than for the same system at zero field, which is consistent with the slight shift of the melting peak toward high temperatures as the external field strength is increased in Figs. 1(e) and 1(f).

To quantify the diversity of structures in the IS analysis, the information entropy S_{IS} extracted from the populations $\{p_\alpha\}$ of conformers was determined as a function of temperature. The variations of this quantity with temperature are shown in Fig. 3 for the same clusters having 8 or 27 particles and the same external field strengths, thus allowing a direct comparison with the other equilibrium properties represented in Fig. 1.

For the two systems, the information entropy vanishes in the low-temperature limit and independently of the external field strength. As soon as some isomerization takes place, S_{IS} increases either monotonically (M_8 at low and high field) or exhibits local maxima at the same temperatures at which the heat capacity shows premelting maxima as well. The melting peak itself is associated with the greater increase in S_{IS}, which coincides with the appearance of new bunches of conformers as seen in the IS spectra of Fig. 2. What the information entropy demonstrates clearly is, precisely, the entropic nature of some structural transitions, such as the one occuring below $T = 1$ for M_{27} at high field $B = 0.9$. Inspection of the heat capacity or other properties does not discriminate between specific conformers, while S_{IS} drops to zero between $T = 1$ and $T \simeq 3$ for this system, showing unambiguously that a single structure is visited, with maximum gyration radius and strong magnetization: the linear chain.

For a given system, decreasing the external field generally leads to a higher information entropy once the melted state is reached. This apparently greater diversity of inherent structures, also noted in the IS spectra of Fig. 2, mostly reflects the statistical preference for conformers with a higher total dipole moment and the relative destabilization of remaining conformers.

Having characterized structural transitions from dedicated parameters, and using the detailed information provided by the inherent structures, some tentative phase diagrams can be constructed as a dual function of temperature and external magnetic field and for selected sizes. Such diagrams are represented in Fig. 4 for the three clusters already discussed for M_8, M_{14}, and M_{27} but also for M_{21}. Due to the limited
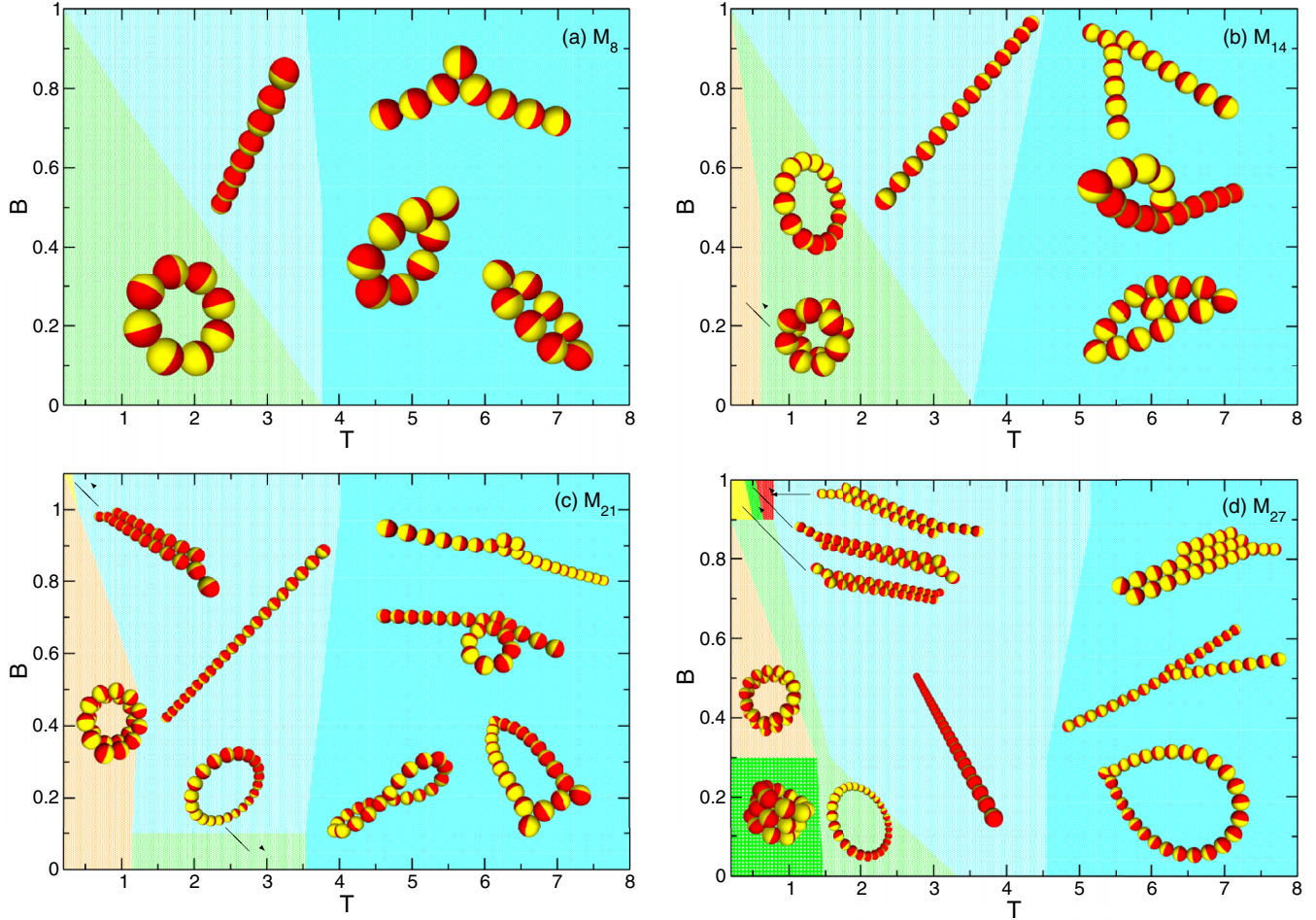
FIG. 4. Structural phase diagrams in the (temperature, field strength) plane highlighting the dominant configurations adopted by selected colloidal clusters. (a) M_8; (b) M_{14}; (c) M_{21}; (d) M_{27}.

number of simulations at finite external field, the boundaries of each colored region are approximate, but generic behaviors common to all system sizes can be clearly delineated.

The most compact configurations that consist of single (M_8) or stacked (M_n with $n = 14$, 21, 27) rings are only predominant at low temperature *and* field. Increasing temperature at low field invariably leads to entropy-driven structural transitions toward the single-ring conformer and subsequently to chains that have even higher entropy due to their much softer vibrational modes. Chains are also stabilized by increasing the external field, the energy (and global dipole moment) being maximized by aligning the dipole moments with the field.

In larger clusters (M_{21} and M_{27} here) intermediate two-chain conformations are found to be the most stable at high field, but single-chain structures should become favored at even higher fields not explored here. In the largest cluster considered, several two-chain conformations also coexist with some minor dependence on temperature. The stability region of the single chain conformer is bounded both at low and high temperatures and broadens with increasing external field. However, at any field a melting phase change takes place at sufficiently high temperature, above which entropic disorder prevails over the ordering ability of the field. The melted phase itself can be better visualized from the

inherent structures superimposed on the diagrams, selected for each cluster to illustrate the variety of shapes that are visited.

These structures obviously differ markedly from the highly symmetric, low-energy ring conformers and contain typical defect motifs that are common to all system sizes: rings with one or several necks, multiple chains joined at the center, nonplanar rings, or even rather compact, two-dimensional (2D) sheet fragments. Due to the high temperature and frequent rearrangements, none of these conformers is expected to be long lived, and this diversity of structures only has a statistical meaning. Moreover, because we have restricted configuration space to be connected structures only, any experimental realization would have to prevent thermal dissociation as well in order to monitor specific structures.

IV. DISCUSSION AND CONCLUSIONS

Clusters of magnetic colloidal particles have already been experimentally produced by several groups and shown to exhibit propensity for self-assembly. Controlling the shape of these clusters appears primarily feasible by appropriate tuning of their interactions, either through the shape of individual particles (which influences the range of the interaction) or through the magnitude of the dipole moment (which influences

the anisotropy more directly). Altering cluster shapes by external parameters such as magnetic field or temperature would pave the way toward additional or improved control for possible applications.

In the limits of low field and low temperature, compact shapes are generally favored with no net dipole moment. In the size range considered here with at most 27 particles, these compact shapes generally consist of superimposed rings, but with the present parameters the lowest-energy structure was predicted to be even more compact and based on the face-centered-cubic crystal [40].

The single chain is expected to become the only stable conformer at sufficiently high field. Conversely, increasing the temperature should favor structural diversity and a melted (fluxional) phase. It would be interesting to determine which of the two parameters of field and temperature dominates over the other in the limit where they both take large values or, in other terms, whether it is possible to stabilize the single chain structure by increasing the field even if the temperature is high.

Another general finding is the stabilization of single ring conformers by entropy at intermediate temperatures and low field, and the systematic structural transition to the single chain structure (opening of the ring) on increasing the field. The very large entropy of the single ring conformer, which conveys very floppy out-of-plane modes, is reflected on the inherent structure entropy that exhibits nonmonotonic variations with increasing temperature when such transitions take place, possibly even dropping to zero before increasing again.

Obviously, clusters with arbitrary sizes other than those scrutinized here should display quantitatively different caloric curves but a similar phenomenology is expected. In particular, the ring and chain conformers will remain as highly stable structures at intermediate temperatures and low and high fields, respectively, while structures based on multiple rings will depend on the precise number of particles forming the individual rings. Preliminary calculations on the larger cluster M_{36} with a fcc global minimum suggest an additional structural transition toward multiple ring conformers before fewer but larger rings, chains, and eventually the fluxional phase take place.

The multiple structural transitions found for the present systems bear strong similarities with the multistep melting process reported earlier in atomic and molecular clusters both theoretically [47–50] and experimentally [51], and especially the hierarchical melting found for ionic aggregates [52,53], in which the presence of several features in the caloric curves is related to the successive opening of broader regions of the energy landscape.

Among the questions raised by the present results, the robustness of the structural transitions and phase boundaries against the details of the model would be worth pursuing in the future, not only in terms of parameter values but also and more generally of the potential itself. One approximation made in the model was notably that the dipole strength is independent of temperature, which for many magnetic materials could be disputable. Extending the model to include temperature-dependent dipole moments would still be straightforward in the present framework. This work and the underlying model could also be employed in two dimensions, either without environment or in the presence of an explicit substrate that mimics the actual confinement. Although the presence and mechanisms of structural and phase changes could be preserved in 2D, the further constraints on the vibrational modes could significantly reduce the entropic stabilization of single-ring and -chain conformers, while favoring more compact hexagonal packings. Future work could also address the even more complex case of bi- or polydisperse clusters having particles of different size or carrying dipoles with different magnitude or with off-centered dipole moments. In addition to structural complexity, the phase diagram could then exhibit competing isomers that differ not in shape but in the arrangement of unlike particles, producing new structures or reducing their numbers.

All transitions explored in the present investigation being at thermal equilibrium, another relevant issue would be to consider their kinetics and in particular the time scales associated with the ring $\rightleftharpoons$ chain interconversion but also the more complex rearrangements between the different branched structures and the more compact multiple ring conformers. Recent work using Langevin molecular dynamics [29] could shed light onto some aspects of these transitions, but a more systematic approach based on path sampling techniques [54,55] would probably be more appropriate to reach macroscopically long time scales.

ACKNOWLEDGMENTS

[1] W. Wen, F. Kun, K. F. Pál, D. W. Zheng, and K. N. Tu, Aggregation kinetics and stability of structures formed by magnetic microspheres, Phys. Rev. E **59**, R4758 (1999).

[2] F. Kun, W. Wen, K. F. Pál, and K. N. Tu, Breakup of dipolar rings under a perpendicular magnetic field, Phys. Rev. E **64**, 061503 (2001).

[3] G. M. Whitesides and B. Grzybowski, Self-assembly at all scales, Science **295**, 2418 (2002).

[4] H. Zeng, J. Li, J. P. Liu, Z. L. Wang, and S. Sun, Exchange-coupled nanocomposite magnets by nanoparticle self-assembly, Nature (London) **420**, 395 (2002).

[5] J. M. Perez, F. J. Simeone, Y. Saeki, L. Josephson, and R. Weissleder, Viral-induced self-assembly of magnetic nanoparticles allows the detection of viral particles in biological media, J. Am. Chem. Soc. **125**, 10192 (2003).

[6] K. Butter, P. H. H. Bomans, P. M. Frederik, G. J. Vroege, and A. P. Philipse, Direct observation of dipolar chains in iron ferrofluids by cryogenic electron microscopy, Nat. Mater. **2**, 88 (2003).

[7] S. L. Tripp, R. E. Dunin-Borkowski, and A. Wei, Flux closure in self-assembled cobalt nanoparticle rings, Angew. Chem., Int. Ed. Engl. **115**, 5749 (2003).

[8] H. Morimoto, T. Maekawa, and Y. Matsumoto, Statistical analysis of two-dimensional cluster structures composed of ferromagnetic particles based on a flexible chain model, Phys. Rev. E **68**, 061505 (2003).

[9] M. Klokkenburg, C. Vonk, E. M. Claesson, J. D. Meeldijk, B. H. Erné, and A. P. Philipse, Direct imaging of zero-field dipolar structures in colloidal dispersions of synthetic magnetite, J. Am. Chem. Soc. **126**, 16706 (2004).

[10] M. A. Miller and D. J. Wales, Novel structural motifs in clusters of dipolar spheres: Knots, links, and coils, J. Phys. Chem. B **109**, 23109 (2005).

[11] A. Snezhko, I. S. Aranson, and W.-K. Kwok, Structure Formation in Electromagnetically Driven Granular Media, Phys. Rev. Lett. **94**, 108002 (2005).

[12] A. Snezhko, I. S. Aranson, and W.-K. Kwok, Dynamic self-assembly of magnetic particles on the fluid interface: Surface-wave-mediated effective magnetic exchange, Phys. Rev. E **73**, 041306 (2006).

[13] A. Hucht, S. Buschmann, and P. Entel, Molecular dynamics simulations of the dipolar-induced formation of magnetic nanochains and nanorings, Europhys. Lett. **77**, 57003 (2007).

[14] L. Baraban, D. Makarov, M. Albrecht, N. Rivier, P. Leiderer, and A. Erbe, Frustration-induced magic number clusters of colloidal magnetic particles, Phys. Rev. E **77**, 031407 (2008).

[15] H. Morimoto, K. Katano, and T. Maekawa, Ring-chain structural transitions in a ferromagnetic particles system induced by a dc magnetic field, J. Chem. Phys. **131**, 034905 (2009).

[16] N. Osterman, I. Poberaj, J. Dobnikar, D. Frenkel, P. Ziherl, and D. Babić, Field-Induced Self-Assembly of Suspended Colloidal Membranes, Phys. Rev. Lett. **103**, 228301 (2009).

[17] J. Ku, D. M. Aruguete, A. P. Alivisatos, and P. L. Geissler, Self-assembly of magnetic nanoparticles in evaporating solution, J. Am. Chem. Soc. **133**, 838 (2011).

[18] A. Snezhko and I. S. Aranson, Magnetic manipulation of self-assembled colloidal asters, Nat. Mater. **10**, 698 (2011).

[19] J. D. Farrell, C. Lines, J. J. Shepherd, D. Chakrabarti, M. A. Miller, and D. J. Wales, Energy landscapes, structural topologies and rearrangement mechanisms in clusters of dipolar particles, Soft Matter **9**, 5407 (2013).

[20] A. A. Abrikosov, S. Sacanna, A. P. Philipse, and P. Linse, Self-assembly of spherical colloidal particles with off-centered magnetic dipoles, Soft Matter **9**, 8904 (2013).

[21] J. E. Martin and A. Snezhko, Driving self-assembly and emergent dynamics in colloidal suspensions by time-dependent magnetic fields, Rep. Prog. Phys. **76**, 126601 (2013).

[22] R. Messina, L. A. Khalil, and I. Stanković, Self-assembly of magnetic balls: From chains to tubes, Phys. Rev. E **89**, 011202 (2014).

[23] G. Singh, H. Chan, A. Baskin, E. Gelman, N. Repnin, P. Král, and R. Klajn, Self-assembly of magnetite nanocubes into helical superstructures, Science **345**, 1149 (2014).

[24] R. Messina and I. Stanković, Self-assembly of magnetic spheres in two dimensions: The relevance of onion-like structures, Europhys. Lett. **110**, 46003 (2015).

[25] D. Morphew and D. Chakrabarti, Hierarchical self-assembly of colloidal magnetic particles into reconfigurable spherical structures, Nanoscale **7**, 8343 (2015).

[26] D. Morphew and D. Chakrabarti, Supracolloidal reconfigurable polyhedra via hierarchical self-assembly, Soft Matter **12**, 9633 (2016).

[27] D. Morphew and D. Chakrabarti, Clusters of anisotropic colloidal particles: From colloidal molecules to supracolloidal structures, Curr. Opin. Colloid Interface **30**, 70 (2017).

[28] R. Messina and I. Stanković, Assembly of magnetic spheres in strong homogeneous magnetic field, Physica A (Amsterdam) **466**, 10 (2017).

[29] E. V. Novak, D. A. Rozhkov, P. A. Sanchez, and S. S. Kantorovich, Self-assembly of designed supramolecular magnetic filaments of different shapes, J. Magn. Magn. Mater. **431**, 152 (2017).

[30] D. Zerrouki, J. Baudry, D. Pine, P. Chaikin, and J. Bibette, Chiral colloidal clusters, Nature (London) **455**, 380 (2008).

[31] R. W. Perry, G. Meng, T. G. Dimiduk, J. Fung, and V. N. Manoharan, Real-space studies of the structure and dynamics of self-assembled colloidal clusters, Faraday Discuss. **159**, 211 (2012).

[32] D. Vella, E. du Pontavice, C. L. Hall, and A. Goriely, The magneto-elastica: From self-buckling to self-assembly, Proc. R. Soc. Lond. A **470**, 20130609 (2013).

[33] G. Meng, N. Arkus, M. P. Brenner, and V. N. Manoharan, The free-energy landscape of clusters of attractive hard spheres, Science **327**, 560 (2010).

[34] Q. Chen, J. K. Whitmer, S. Jiang, S. C. Bae, E. Luijten, and S. Granick, Supracolloidal reaction kinetics of Janus spheres, Science **331**, 199 (2011).

[35] P. J. Yunker, K. Chen, Z. Zhang, and A. G. Yodh, Phonon Spectra, Nearest Neighbors, and Mechanical Stability of Disordered Colloidal Clusters with Attractive Interactions, Phys. Rev. Lett. **106**, 225503 (2011).

[36] C. L. Klix, K. Murata, H. Tanaka, S. R. Williams, A. Malins, and C. P. Royall, Novel kinetic trapping in charged colloidal clusters due to self-induced surface charge organization, Sci. Rep. **3**, 2072 (2013).

[37] N. Vandewalle and S. Dorbolo, Magnetic ghosts and monopoles, New J. Phys. **16**, 013050 (2014).

[38] C. Holm and J.-J. Weis, The structure of ferrofluids: A status report, Curr. Opin. Colloid Interface Sci. **10**, 133 (2005).

[39] L. Rovigatti, J. Russo, and F. Sciortino, No Evidence of Gas-Liquid Coexistence in Dipolar Hard Spheres, Phys. Rev. Lett. **107**, 237801 (2011).

[40] J. Hernández-Rojas, D. Chakrabarti, and D. J. Wales, Self-assembly of colloidal magnetic particles: Energy landscapes and structural transitions, Phys. Chem. Chem. Phys. **18**, 26579 (2016).

[41] R. H. Swendsen and J.-S. Wang, Replica Monte Carlo Simulation of Spin-Glasses, Phys. Rev. Lett. **57**, 2607 (1986).

[42] F. Calvo and P. Dugourd, Folding of gas-phase polyalanines in a static electric field: Alignment, deformations, and polarization effects, Biophys. J. **95**, 18 (2008).

[43] D. J. Wales, *Energy Landscapes* (Cambridge University Press, Cambridge, 2003).

[44] J. Nocedal, Updating quasi-Newton matrices with limited storage, Math. Comput. **35**, 773 (1980).

[45] D. Liu and J. Nocedal, On the limited memory BFGS method for large scale optimization, Math. Programming **45**, 503 (1989).

[46] D. J. Wales, The energy landscape as a unifying theme in molecular science, Philos. Trans. R. Soc. Lond. A **363**, 357 (2005).

[47] R. Poteau, F. Spiegelmann, and P. Labastie, Isomerisation and phase transitions in small sodium clusters, Z. Phys. D **30**, 57 (1994).

[48] J. P. K. Doye and D. J. Wales, Thermodynamics of Global Optimization, Phys. Rev. Lett. **80**, 1357 (1998).

[49] F. Calvo and F. Spiegelmann, Geometric Size Effects in the Melting of Sodium Clusters, Phys. Rev. Lett. **82**, 2270 (1999).

[50] D. D. Frantz, Magic number behavior for heat capacities of medium-sized classical Lennard-Jones clusters, J. Chem. Phys. **115**, 6136 (2002).

[51] G. A. Breaux, C. M. Neal, B. Cao, and M. F. Jarrold, Melting, Pre-Melting, and Structural Transitions in Size-Selected Aluminum Clusters with Around 55 Atoms, Phys. Rev. Lett. **94**, 173401 (2005).

[52] J. Luo, U. Landman, and J. Jortner, in *Physics and Chemistry of Small Clusters*; NATO ASI Series B, Vol. 158, edited by P. Jena, B. K. Rao, and S. Khanna (Plenum, New York, 1987), p. 155.

[53] F. Calvo and P. Labastie, Melting and phase space transitions in small ionic clusters, J. Phys. Chem. B **102**, 2051 (1998).

[54] P. G. Bolhuis, D. Chandler, C. Dellago, and P. L. Geissler, Transition path sampling: Throwing ropes over rough mountain passes, in the dark, Annu. Rev. Phys. Chem. **53**, 291 (2002).

[55] D. J. Wales, Discrete path sampling, Mol. Phys. **100**, 3285 (2002).